

# International Conference on Space Optics—ICSO 2010

Rhodes Island, Greece

4–8 October 2010

*Edited by Errico Armandillo, Bruno Cugny,  
and Nikos Karafolas*



## *First results of the PERSEE experiment*

*J.-M. Le Duigou, J. Lozi, F. Cassaing, K. Houairi, et al.*



International Conference on Space Optics — ICSO 2010, edited by Errico Armandillo, Bruno Cugny,  
Nikos Karafolas, Proc. of SPIE Vol. 10565, 105650W · © 2010 ESA and CNES  
CCC code: 0277-786X/17/\$18 · doi: 10.1117/12.2309159

## FIRST RESULTS OF THE PERSEE EXPERIMENT

J.M. Le Duigou<sup>1</sup>, J. Lozi<sup>2,3</sup>, F. Cassaing<sup>2,3</sup>, K. Houairi<sup>2,3</sup>, B. Sorrente<sup>2,3</sup>, J. Montri<sup>2,3</sup>,  
S. Jacquinod<sup>4</sup>, J-M Reess<sup>5,2</sup>, L. Pham<sup>5,2</sup>, E. Lhomé<sup>5,2</sup>, T. Buey<sup>5,2</sup>, F. Hénault<sup>6</sup>, A. Marcotto<sup>6</sup>,  
P. Girard<sup>6</sup>, N. Mauclet<sup>6</sup>, M. Barillot<sup>7</sup>, V. Coudé du Foresto<sup>5,2</sup> and M. Ollivier<sup>4</sup>

<sup>1</sup> Centre National d'Etudes Spatiale  
18 Avenue Edouard Belin  
31401 TOULOUSE Cedex 9 – France  
tel : (+33) 1 61 28 21 24  
fax : (+33) 1 61 28 26 92

[Jean-Michel.LeDuigou@cnes.fr](mailto:Jean-Michel.LeDuigou@cnes.fr)

<sup>2</sup> Office National d'Etudes et de Recherches Aérospatiales

<sup>3</sup> Groupement d'Intérêt Scientifique PHASE (Partenariat Haute résolution Angulaire Sol Espace)

<sup>4</sup> Institut d'Astrophysique Spatiale d'ORSAY

<sup>5</sup> Observatoire de Paris

<sup>6</sup> : Observatoire de la Côte d'Azur

<sup>7</sup> : Thalès Alénia Space

### 1. INTRODUCTION

Although it has been recently postponed due to high cost and risks, nulling interferometry in space remains one of the very few direct detection methods able to characterize extrasolar planets and particularly telluric ones. Within this framework, several projects such as DARWIN [1], [2], TPF-I [3], [4], FKSI [5] or PEGASE [6], [7], have been proposed in the past years. Most of them are based on a free flying concept. It allows firstly to avoid atmosphere turbulence, and secondly to distribute instrumental function over many satellites flying in close formation. In this way, a very high angular resolution can be achieved with an acceptable launch mass. But the price to pay is to very precisely position and stabilize relatively the spacecrafts, in order to achieve a deep and stable extinction of the star. Understanding and mastering all these requirements are great challenges and key issues towards the feasibility of these missions. Thus, we decided to experimentally study this question and focus on some possible simplifications of the concept.

Since 2006, PERSEE (PEGASE Experiment for Research and Stabilization of Extreme Extinction) laboratory test bench is under development by a consortium composed of Centre National d'Etudes Spatiales (CNES), Institut d'Astrophysique Spatiale (IAS), Observatoire de Paris-Meudon (LESIA), Observatoire de la Côte d'Azur (OCA), Office National d'Etudes et de Recherches Aérospatiales (ONERA), and Thalès Alénia Space (TAS) [8]. It is mainly funded by CNES R&D. PERSEE couples an infrared wide band nulling interferometer with local OPD and tip/tilt control loops and a free flying Guidance Navigation and Control (GNC) simulator able to introduce realistic disturbances. Although it was designed in the framework of the PEGASE free flying space mission, PERSEE can adapt very easily to other contexts like FKSI (in space, with a 10 m long beam structure) or ALADDIN [9] (on ground, in Antarctica) because the optical designs of all those missions are very similar. After a short description of the experimental setup, we will present first the results obtained in an intermediate configuration with monochromatic light. Then we will present some preliminary results with polychromatic light. Last, we discuss some very first more general lessons we can already learn from this experiment.

### 2. PERSEE SHORT DESCRIPTION

This section provides the reader with a very brief description of PERSEE. Much more details can be obtained by the interested reader from [8], [10]–[12].

#### *A PERSEE goals*

The goal of PERSEE is not to reach the deepest possible nulling. Starting from a state of the art nuller of the 2006-2007 period, it is an experimental attempt to better master the system flowdown of the nulling requirements both at payload (instrument main optical bench) and platform levels (satellites). The balance of the constraints between those two levels is a key issue. The more disturbances the payload can face, the simpler the platforms are, the lower the cost. The general idea is hence to simplify as much as possible the global design and reduce the costs of a possible future space mission.

The detailed objectives have been described in [8]. Our main requirement is to reach a  $10^{-4}$  nulling ratio in the [1.65-2.4]  $\mu\text{m}$  band (40% spectral bandwidth) with a  $10^{-5}$  stability over a 10 h time scale. Another important requirement is to be able to find and stabilize fringes which have an initial drift speed (as seen from the

interferometer core) up to 150  $\mu\text{m/s}$ , as this can greatly simplify the relative metrology and control needs. We want to study and maximize the rejection of external disturbances introduced at relevant degrees of freedom of the optical setup by a disturbance module simulating various environments coming from the platform level.

*B Optical setup general description*

Fig. 1 gives an overview of the optical layout. The source module combines various light sources in order to simulate a star light in a wide spectral range. All sources are injected into single-mode fibers which outputs are grouped together at the focus of a collimator. The I channel ( $[0.8-1] \mu\text{m}$ ) is dedicated to the Fringe Sensor (FS) and the Field Relative Angle Sensor (FRAS). The J channel ( $[1-1.5] \mu\text{m}$ ) is dedicated to the FS only. The nulling rate is measured in the K band ( $[1.65-2.4] \mu\text{m}$ ). The 40 mm beams coming out of the separation module first encounter two  $45^\circ$  fold mirrors (M1) simulating siderostats. Accurate calibrated perturbations can be introduced at this level either in tip/tilt (few tens of mas resolution) or OPD (nm resolution). The optical train incorporates then afocal systems with  $M = 3$  magnification to reduce the beam size down to about 13 mm. M4 mirrors deviate the beam toward the -Z direction. Coupled with the M1 mirrors, they create a “field reversal” achromatic phase shift between the two arms [13]. Following, each arm has a cat’s eye delay line (50 mm stroke and 10 nm resolution) and a  $30^\circ$  active M6 mirror acting both in tip/tilt and fine OPD (0.2 nm resolution). These active systems can all together generate various corrections covering the necessary range and resolution both in tip/tilt and OPD. They are used in dedicated control loops which use the FRAS camera for the tip/tilt and the FS for the OPD. L1 and L2, located just before the combining stage, are an optional phase shift compensator.

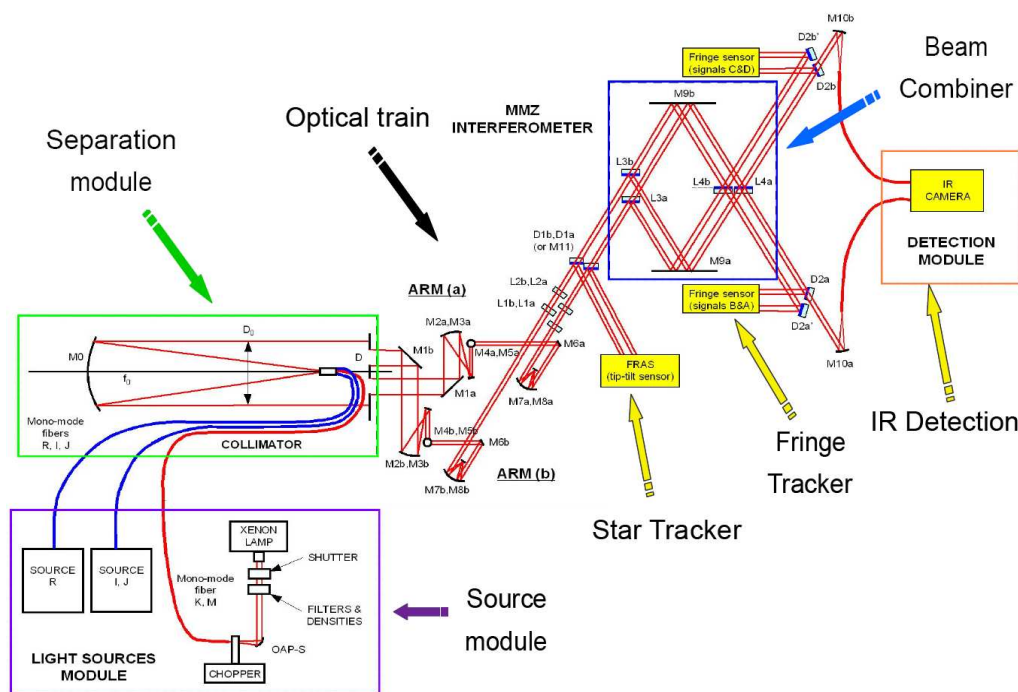


**Fig. 1.** General setup of PERSEE in the final operational state.

The combining stage is a kind of Modified Mach-Zehnder (MMZ) [13] with two inputs (a and b arms) and four outputs (I to IV). Due to some symmetry and optical tight tolerances, the setup guarantees that two outputs are achromatic. The four beam splitters have a trapezoidal geometry [11] to avoid stray light. They have a specifically designed three-layer coating of about 200 nm thickness which allows to achieve appropriate reflection and transmission coefficients for both polarizations in the whole K band. The beam splitters are divided into two groups as compared to the classical setup [13]. This allow to translate L3a component without impacting the nulling output (output III). The translation is adjusted so that the four outputs generate four points in the I and J fringes roughly with a  $\lambda/4$  spacing, which allows a spatial ABCD fringe tracking algorithm. The tip/tilt degrees of freedom of L3a are used to maximize the contrast in the FS A and C outputs (I and IV). This compact design allows to minimize differential optical path between FS and nulled output down to about 10 cm. This point is critical because it relaxes the stabilization requirements at system level.

After the MMZ, dichroic plates separate the various spectral channels and direct them into appropriate detection chains via injection into optical fibers. The FS detection is made of a set of eight monopixels and multimode fibers. For the K channel, the light is injected in a fluoride glass single mode fiber. The detector is a cooled infrared camera based on a Teledyne picnic matrix behind a dispersive element which allows to have polychromatic measurements of both dark and bright fringes at the same time. A calibrated optical attenuator is used in the bright output to optimize the dynamic of both outputs with respect to the detector well depth.

### 3. RESULTS IN MONOCHROMATIC CONFIGURATION

#### A Autocollimation setup

As PERSEE is a quite complex breadboard with many components, the integration was made progressively using many intermediate steps. The most important one at the start of the process was a so-called “autocollimation setup” illustrated by Fig. 2.

In this phase, we focused on the MMZ and the FS performances associated to a monochromatic nulled output measured by a single-pixel infrared detector. The several light sources were injected from some outputs and reflected back to inputs of the combination stage by the two M6 mirrors. The I channel used a fibered DFB laser diode at 830 nm leading to a very long coherence length. It was injected in output II with a dedicated injection. The J channel used a SLED at 1320 nm with 40 nm spectral width leading to a coherence envelope of about 40  $\mu\text{m}$ . It was injected in the reception fiber of output III. In the K channel, a DFB laser diode at 2320 nm was injected through a fluoride glass single mode fiber in output III. This setup had some drawbacks: by instance, the I flux in output III and IV were not balanced, contrary to the final setup. Furthermore, as an output was occupied by J source, the algorithm in this band was adapted to an ABC modulation.

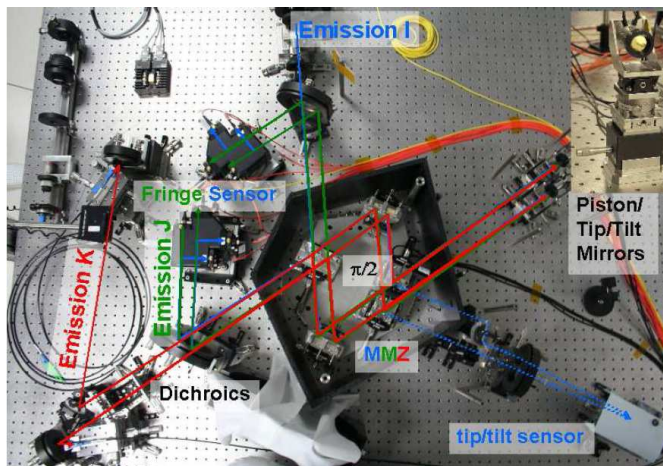


Fig.2. Autocollimation setup.

#### B Analysis of laboratory disturbances on OPD measurement

One of PERSEE goals is to cophase the two beams to a nanometric level, so it is very sensitive to laboratory disturbances, like thermal drifts, acoustic or mechanical vibrations.

Fig. 3 (left) compares the drift of outputs I and IV versus output II and III, and the temperature variations of a beam splitter inside the MMZ during 3 days. The correlation factor in that configuration is 1200 nm/K. In autocollimation, the light passes twice through the interferometer. So in the complete setup, that factor will be halved: 600 nm/K. This instability comes mainly from the standard mechanical mounts of the optics made of aluminium and steel. Specially designed more stable mounts were studied but could not be afforded by the project. This internal drift results in some slow variations of the modulation matrix coefficients. From the four outputs measurements, this matrix allows to calculate in real-time the flux in each arm, the visibility and the OPD either in the I or J channel. The thermal drifts are compensated by regular calibrations of the modulation matrix using open loop calibrated fast movements of the M6 mirrors (few seconds every half an hour).

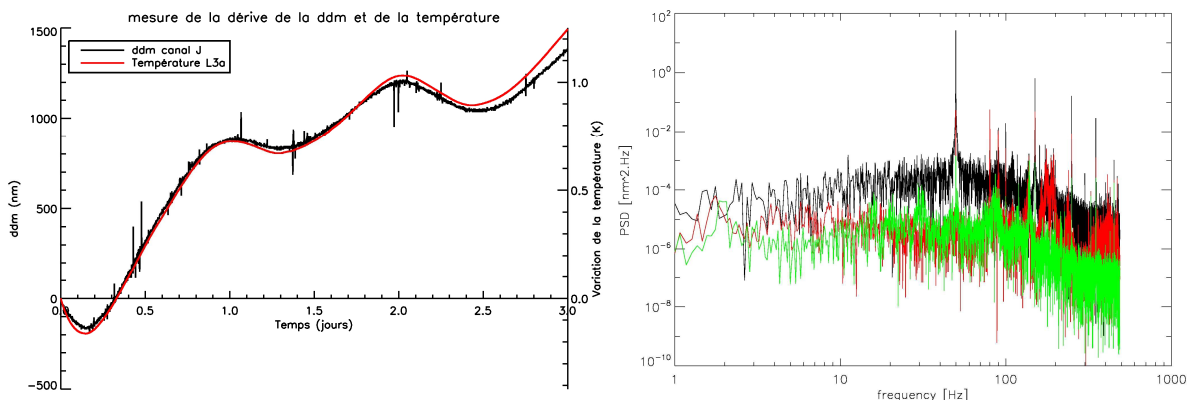


Fig. 3. OPD between outputs IV and III and temperature variations vs time (left). PSD of OPD with piezo strain gauges (black), w/o gauges (red), w/o gauges and other acoustic disturbances (green), (right).

Fig. 3 (right) shows steps of noise reduction on the PSD of the OPD. The impact of piezo strain gauges is visible in a strong vibration at 50 Hz and a stronger white noise. By turning them off, we reduce significantly the noise, but there are still strong contributions around 80, 130 and 170 Hz. Those are mechanical vibrations: the M6

mirror assembly for the 80 Hz, and the MMZ for the 130 and 170 Hz. By deporting all electronic devices out of the room, and by turning off the A/C, we suppress every acoustic noise perturber. Thereby, we reduce those mechanical vibrations. Nevertheless there are still some residues, of about 1 nm rms that we will have to manage with the appropriate control law. The monochromatic results show that the two main contributors for the nulling rate are the photometric unbalance and the OPD noise.

### C Best results in the autocollimation setup

In the best conditions, we cophased the two beams with a standard deviation of  $\sigma_{OPD} = 0.22 \text{ nm in OPD}$  (at 1 kHz during 10 s) and  $\sigma_{tip/tilt} = 60 \text{ mas}$  in tip/tilt (at 200 Hz during 10 s). In that setup, we obtained regularly that value of  $\sigma_{tip/tilt}$ , and better than 0.4 nm in OPD. In tip/tilt, the performances are limited by the measurement noise, contrary to the OPD performances, which are limited by laboratory disturbances. Data were acquired during 10 s, but results are very similar for 100 s time scales. 100 s is the typical duration between adjustments of satellite trajectories in the PEGASE mission framework. For the monochromatic nulling rate at  $2.32 \mu\text{m}$ , we achieved an extinction of  $N = 3 \cdot 10^{-5} \pm 3 \cdot 10^{-6}$  at 1 kHz during 100 s. This result is quite reproducible and is very comforting for the following polychromatic step.

## 4. FIRST RESULTS IN POLYCHROMATIC CONFIGURATION

All the following results are preliminary and were obtained in a non optimized configuration and without active opd and tip/tilt control.

### A Setup

These tests were performed in a nearly complete configuration of the bench. Only afocal systems are missing. They were conducted to validate a supercontinuum source that will eventually replace the black body and the two lasers described in section 3.1. The images shown in Fig. 4 were obtained by the low noise nitrogen-cooled camera. The upper row is output III, corresponding to the dark output, imaged through a bi-prism which disperses wavelengths. The lower row is output II, corresponding to the bright output. Each output is dispersed horizontally ( $1.6$  to  $2.3 \mu\text{m}$  on 11 pixels). In that setup, the supercontinuum source is used for both metrology and nulling measurement. The range of metrology is then quite limited by the coherence lengths of the two spectral bands, shorter than those of the SLED and the DFB diode previously used.

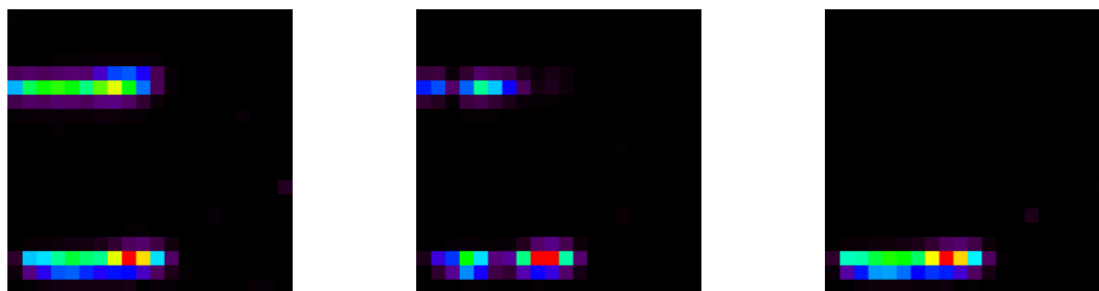


**Fig. 4.** Images of the camera: one arm only (left), interferences at  $OPD \sim 10 \mu\text{m}$  (center), interferences at  $OPD = 0$  (right). The upper row is output III (dark output) and the lower row is output II (bright output).

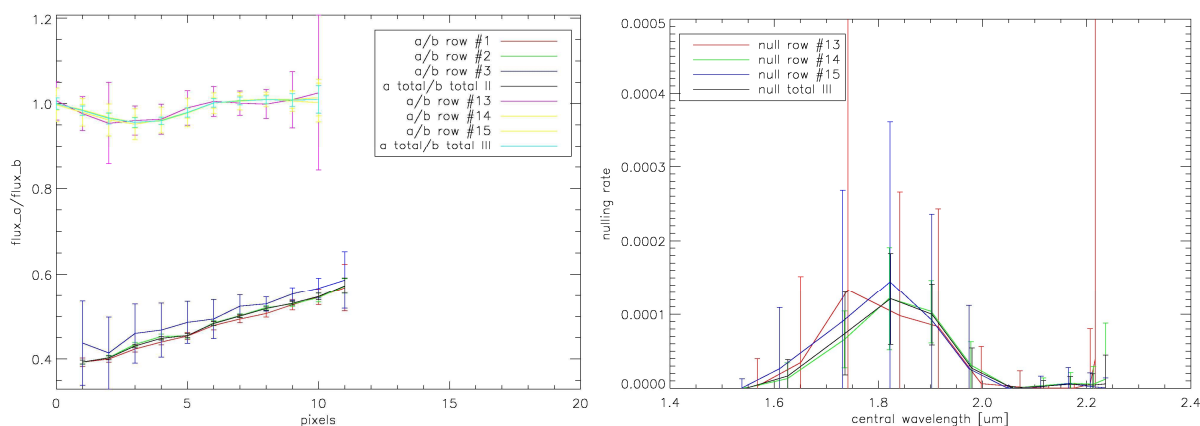


**Fig. 5.** Ratio between flux in arm a and b (left) and theoretical impact on null depth (right).

### B Photometry

We acquire the flux in each arm and for each spectral channel of the camera. Fig. 5 (left), shows the ratio between the two arms. The flux in output III is well balanced (near 1.0 value), unlike in output II (near 0.5 value). This is consistent with the MMZ design. The spectrally averaged photometric unbalance is 1.2%. But there is a visible chromatic effect on this value, maybe due to a misalignment of the bench, or injection in single mode fibers. Locally, the unbalance reaches 5%, with a corresponding nulling of  $10^{-4}$  as illustrated on Fig. 5 (right). After optimization, the flux unbalance should not be a limitation for our  $10^{-4}$  nulling goal.

### C Chromatic effects on OPD

As illustrated by Fig. 6 (left), the nulled output (lower curves) exhibits a 20 nm chromatism between the 1.6 and 2.3  $\mu\text{m}$ . A more detailed analysis shows that a large part of this figure is a linear shift coming from misalignments. This will be corrected later easily either by an improvement of the alignment procedure or by the introduction of a compensator composed of 4 dispersive plates that can manage this kind of error. Fig. 6 (right) shows the minimal chromatic effect that will remain when removing the linear part. This residue is induced by inhomogeneity of coating thickness of beam splitters. A level of a few nm is obtained. It is consistent with what has been simulated for the theoretical study of the bench and compatible with the required nulling level.

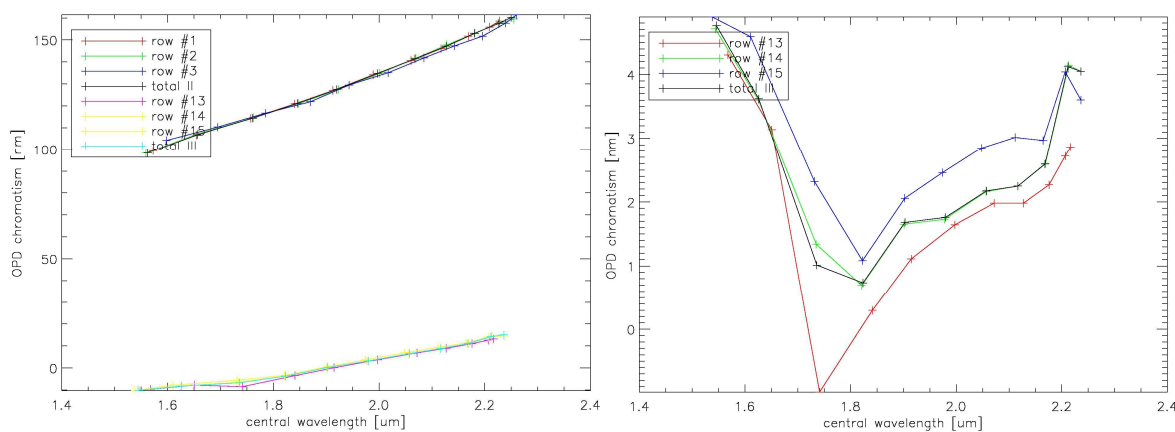


**Fig. 6.** position of fringe minimum for output III and fringe maximum for output II (left) as a function of wavelength. Residual chromatism for output III after linear part removal (right).

### 5.4 Polychromatic nulling rate

We did not perform a real nulling measurement with a stabilized OPD in that configuration (OPD control unavailable in this configuration), but with the data obtained, we can estimate null depth to a few  $10^{-3}$  over the total wavelength range. This very first measured value is quite promising for future works, but need to be improved. The chromatic phase shift is the main error we will have to manage, using the phase shift compensator. That should greatly enhance the quality of the null depth.

## 6. SOME PRACTICAL AND MORE GENERAL FIRST LESSONS

### A Thermal stability

From existing data, we already can infer some general trends and first lessons. By instance, the current MMZ design proved to have a 600 nm/K OPD drift between science and FS channels. In fact, this phenomenon is due to standard mechanics used for supporting the optics and to instability of the mechanism driving the L3a plate. The optics (CaF2) form a nearly auto-compensated optical setup, as the refractive index variations almost compensate the thermoelastic and geometrical effects. An improved MMZ with specially designed optical supports has been considered but could not be afforded in the frame of PERSEE. With sufficient funding, a factor of at least 10 could be saved. This leads to a differential OPD sensitivity of about 50 nm/K. Thus, the thermal stabilization need would be  $\pm 20$  mK on a box of typically 30x30x10 cm size. The rest of the optical bench could be stabilized at 0.1 K or even 1 K (the driving constraint there is in fact the thermal background in the measurement itself, not the mechanical stability). This seems quite affordable in space, even in non L2 orbits. The situation could even be improved by a clever use of the 4 MMZ outputs which might help to correct the drift due to temperature at regular intervals. To conclude, for an intermediate mission like PEGASE, which is not requiring extreme cooling of the detector or the optics, an earth orbit is not totally ruled out, as first assumed in previous studies. This could be a great simplification as compared to a L2 mission, which remains nevertheless necessary for the final full mission.

### *B 1 nm cophasing feasibility*

With existing data, we can prove that cophasing two arms on ground at better than 1 nm rms is feasible on a quite big optical setup in a standard building, but one has to take care to many details. By instance, electronics have to be implemented in an adjacent room to avoid unnecessary noise. The piezoelectric devices can not use their internal strain gauges which introduce too much electrical noise. The stiffness of the mechanical mounts supporting the optics has to be studied with care and a specification of at least 150 Hz for the first mechanical mode seems to us a good rule. Typically, on our bench, the mechanical modes of the optics mounts are located between 80 and 170 Hz and react clearly to acoustic solicitations. The FS design using spatial modulation provides OPD measurements with up to 1 kHz sampling frequency which is extremely useful to implement an adequate compensation of microvibrations for both on ground and in flight perturbations. Concerning filtering of mechanical perturbators on board a space mission, no experimental results are yet available, but the simulations give good hope that harmonic perturbations can be significantly reduced using Kalman filtering. This is a good step toward the feasibility of a satellite pointing system using by instance reaction wheels instead of more complex devices.

### *C Fine pointing*

As far as fine pointing is concerned, a 60 mas stability can be reached at payload level, after the afocal systems. This corresponds to a 1/100th of a pixel with a PSF spread over 4 to 5 pixels. It confirms that this point should not be a problem in the future, as expected. By instance, in the PEGASE case, the requirement is 600 mas in the same optical space, a factor of 10 higher. The use of piezoelectric devices within the payload relaxes the pointing requirements at platform level. The best solution is probably to use a spectral band near 1  $\mu\text{m}$  and collect an annular portion of light in some optic before the combining device, instead of using dichroic plates which would introduce chromatic aberrations and are more difficult to qualify for space use due to the coating. The spacecraft requirements will be directly related to the piezoelectric angular stroke (about  $\pm 100$  arcsec mechanical,  $\pm 200$  arcsec optical) and the total angular magnification of the system (20 to 40 in the case of PEGASE, about 100 - 150 for DARWIN). In the PEGASE case, we can estimate that the required satellite pointing is about 10 arcsec (including residual bias after calibration and stability).

## 7. CONCLUSION

Although we did not reach our full objectives yet, we have already a lot of interesting data and very promising results. 1 nm OPD control and 1% flux unbalance are nearly achieved. The best monochromatic null measured is  $10^{-5} \pm 3 \cdot 10^{-6}$  at 2.32  $\mu\text{m}$ . The wide band nulling is currently limited by chromatic effects. But this issue will be solved soon by the phase shift compensator. Thus, we are quite confident that PERSEE will be optimized before the end of 2010. Then it will enter an exploitation phase where experiments will be carried out by various teams. This phase will be structured by a scientific group which will collect and sort the proposals. At that point, the use of PERSEE will be open to international teams.

## REFERENCES

- [1] Léger, et al., "The DARWIN project," *Astrophysics and Space Science* 241, 135-146 (1996).
- [2] Léger, A., et al., "DARWIN mission proposal to ESA," *ESA's Cosmic Vision Call for Proposals*, (2007).
- [3] Beichman, C. A., et al., "The Terrestrial Planet Finder (TPF) : a NASA Origins Program to search for habitable planets," (1999).
- [4] Lawson, P. R., "Principles of Long Baseline Stellar Interferometry," (2000).
- [5] Danchi, W. C., et al., "Scientific rationale for exoplanet characterization from 3-8 microns: the FKSI mission," *Proc. SPIE* 6268, 626820 (2006).
- [6] Ollivier, M., et al., "Pegase, an infrared interferometer to study stellar environments and low mass companions around nearby stars," *ESA's Cosmic Vision Call for Proposals*, (2007).
- [7] J.M. Le Duigou et al., "Pegase: a space-based nulling interferometer," *Proceedings of the SPIE* 6265, n° 62651M (2006).
- [8] Cassaing, F., et al., "Persee: a nulling demonstrator with real-time correction of external disturbances," *Proc. SPIE* 7013(1), 70131Z (2008).
- [9] Coudé du Foresto, V., et al., "ALADDIN: an optimized nulling ground-based demonstrator for DARWIN," *Proc. SPIE* 6268, 626810 (2006).
- [10] Houairi, K., et al., "PERSEE, the dynamic nulling demonstrator: Recent progress on the cophasing system," *Proc. SPIE*, (2008).
- [11] Jacquinod, S., et al., "PERSEE: description of a new concept for nulling interferometry recombination and opd measurement," *Proc. SPIE* 7013, (2008).
- [12] Hénault, F., et al., "Review of OCA activities on nulling testbench PERSEE," *Proc. SPIE* 7734, (2010).
- [13] Serabyn, E., et al., "Fully symmetric nulling beam combiners," *Appl. Opt.* 40(10), 1668-1671 (2001).